Available online at www.sciencedirect.com
ScienceDirect
International Journal of Solids and Structures 44 (2007) 1939–1948
INTERNATIONAL JOURNAL OF SOLIDS and STRUCTURES
www.elsevier.com/locate/ijsolstr

Non-slipping adhesive contact between mismatched elastic cylinders

Shaohua Chen [a], Huajian Gao [b,*]

[a] LNM, Institute of Mechanics, Chinese Academy of Sciences, 100080 Beijing, China
[b] Division of Engineering, Brown University, Providence, RI 02912, USA

Received 19 April 2006
Available online 3 August 2006

Guest Editor: T. Nakamura

Abstract

We have recently proposed a generalized JKR model for non-slipping adhesive contact between two elastic spheres subjected to a pair of pulling forces and a mismatch strain (Chen, S., Gao, H., 2006c. Non-slipping adhesive contact between mismatched elastic spheres: a model of adhesion mediated deformation sensor. J. Mech. Phys. Solids 54, 1548–1567). Here we extend this model to adhesion between two mismatched elastic cylinders. The attention is focused on how the mismatch strain affects the contact area and the pull-off force. It is found that there exists a critical mismatch strain at which the contact spontaneously dissociates. The analysis suggests possible mechanisms by which mechanical deformation can affect binding between cells and molecules in biology.

Keywords: Adhesion; Contact; Deformation; JKR model; Biological materials

1. Introduction

The last few decades have witnessed significant progresses in the mechanics of adhesive contact between elastic bodies (Johnson et al., 1971; Derjaguin et al., 1975; Roberts and Thomas, 1975; Muller et al., 1980; Greenwood and Johnson, 1981; Barquins, 1988; Maugis, 1992; Carpick et al., 1996; Chaudhury et al., 1996; Baney and Hui, 1997; Greenwood, 1997; Johnson and Greenwood, 1997; Barthel, 1998; Robbe-Valloire and Barquins, 1998; Greenwood and Johnson, 1998; Kim et al., 1998; Shull, 2002; Morrow et al., 2003; Schwarz, 2003). More recently, various contact mechanics theories have also been developed to understand the basic principles behind hierarchical adhesion structures of gecko and insects (Autumn et al., 2002; Artz et al., 2003; Persson, 2003; Gao and Yao, 2004; Glassmaker et al., 2004; Hui et al., 2004; Gao et al., 2005; Huber et al., 2005; Spolenak et al., 2005; Yao and Gao, 2006). Most of the existing models on contact

* Corresponding author. Tel.: +1 401 8632626.
E-mail address: huajian_Gao@Brown.edu (H. Gao).

0020-7683/$ - see front matter
doi:10.1016/j.ijsolstr.2006.07.021

mechanics have focused on the normal tractions inside the contact region (Johnson, 1985). On the other hand, recent studies on elastic bodies in non-slipping adhesive contact with a laterally stretched substrate (Chen and Gao, 2006a,b) indicate that the substrate strain can have significant effect on the contact area. Further study on the pull-off process of two elastic spheres in non-slipping adhesive contact under a pair of pulling forces and a mismatch strain suggests that the mismatch strain can play a dominant role in adhesion (Chen and Gao, 2006c). For example, as the mismatch strain is increased, the contact area is found to continuously decrease until the contact suddenly breaks off at a critical strain. These studies suggest possible connections to general observations in biology that cells and biomolecules can sense and react to mechanical signals in the environment.

The present paper extends our previous analysis of non-slipping adhesive contact between mismatched elastic spheres (Chen and Gao, 2006c) to the corresponding plane strain problem of contact between elastic cylinders. In contrast to the classical JKR model, we assume that the contact area is perfectly bonded such that both tangential and normal tractions are transmitted across the contact interface. This assumption has been inspired by specific ligand–receptor binding in cell adhesion as well as specific sequence matching in adhesion between biomolecules. If there is one to one bonding between specific molecules, shear deformation along the contact interface would not be easily relaxed. The focus of the present study is on how the mismatch strain influences the contact area and the pull-off force between two adhering cylinders.

2. Model

Fig. 1 shows two dissimilar elastic cylinders that are brought into adhesive contact and then subjected to the combined action of a pair of pulling forces F and a mismatch strain ε. The contact region is assumed to be perfectly bonded except that the edge of contact is allowed to shift according to the changing balance between elastic energy and surface energy in the system.

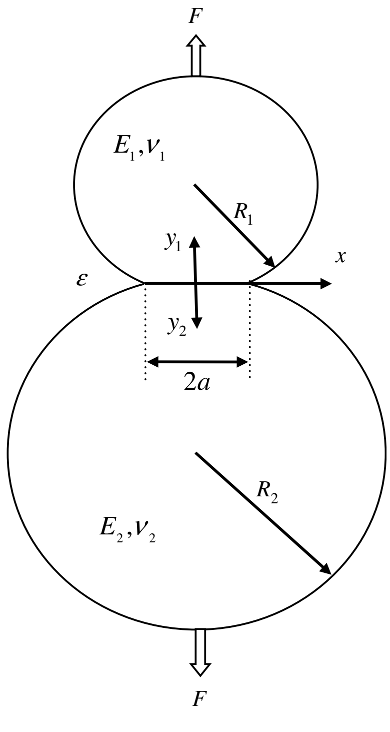

Fig. 1. Schematic of two adhering elastic cylinders acted by a pair of forces F and a mismatch strain ε; (E_1, ν_1), (E_2, ν_2) denote Young's moduli and Poisson's ratio of the cylinders; a is the half-width of the contact region.

A pair of Cartesian coordinates (x, y_1), (x, y_2) are placed at the center of the contact region of each cylinder, with y_1 and y_2 pointing into each corresponding body. The Young's moduli and Poisson ratios of the upper and lower cylinders will be denoted as E_1,v_1 and E_2,v_2, respectively; R_1 and R_2 are the radius of each cylinder; a is the half-width of the contact area; $\sigma_{yy}(x)$ and $\sigma_{xy}(x)$ are the normal and tangential tractions along the contact surface of the upper cylinder inside the contact area. This contact model resembles an external interfacial crack problem under plane strain deformation, in which the stress field near the crack tip is known to exhibit an oscillatory singularity (Rice, 1965; Erdogan, 1965; Westmann, 1965).

3. General solution

Under a mismatch strain (e.g., due to change in pressure or temperature in the environment), the relative tangential displacement and displacement gradient in the adhesion zone satisfy

$$\bar{u}_{x1} - \bar{u}_{x2} = \varepsilon x, \quad \frac{\partial \bar{u}_{x1}}{\partial x} - \frac{\partial \bar{u}_{x2}}{\partial x} = \varepsilon, \quad |x| \leqslant a. \tag{1}$$

The normal tractions in the contact area cause the surface of each body to be displaced parallel to the y_i $(i = 1, 2)$ axis (measured positive into each body) by an amount $\bar{u}_{y1}$ and $\bar{u}_{y2}$. According to the usual parabolic assumption of local contact surfaces (Johnson, 1985),

$$\bar{u}_{y1} + \bar{u}_{y2} = \delta - \frac{x^2}{2R}, \quad \frac{\partial \bar{u}_{y1}}{\partial x} + \frac{\partial \bar{u}_{y2}}{\partial x} = -\frac{x}{R}, \quad |x| \leqslant a, \tag{2}$$

where R is the combined radius defined by $1/R = 1/R_1 + 1/R_2$ and δ is the relative displacement at the center of the contact region.

Using the plane strain elastic Green's functions of half-spaces, the displacement gradients in Eqs. (1) and (2) can be expressed in terms of normal and tangential tractions as

$$\begin{cases} \dfrac{1}{\pi} \displaystyle\int_{-a}^{a} \frac{\sigma_{xy}(s)}{s - x} \mathrm{d}s - \beta \sigma_{yy}(x) = \dfrac{E^* \varepsilon}{2}, \\ \dfrac{1}{\pi} \displaystyle\int_{-a}^{a} \frac{\sigma_{yy}(s)}{s - x} \mathrm{d}s + \beta \sigma_{xy}(x) = -\dfrac{E^* x}{2R}, \end{cases} \quad |x| \leqslant a, \tag{3}$$

where

$$\frac{1}{E^*} = \frac{1 - v_1^2}{E_1} + \frac{1 - v_2^2}{E_2} \tag{4}$$

is the combined Young's modulus and

$$\beta = \frac{E^*}{2} \left\{ \frac{(1 - 2v_1)(1 + v_1)}{E_1} - \frac{(1 - 2v_2)(1 + v_2)}{E_2} \right\} \tag{5}$$

is one of Dundurs' elastic constants for biomaterial systems (Dundurs, 1969).

Eqs. (3) are coupled integral equations for the two unknown tractions $\sigma_{yy}(x)$ and $\sigma_{xy}(x)$. It is convenient to rewrite Eqs. (3) in a matrix form (Chen and Gao, 2006a)

$$\frac{1}{\pi} \int_{-a}^{a} \frac{\boldsymbol{A}}{s - x} \boldsymbol{f}(s) \mathrm{d}s + \boldsymbol{B} \boldsymbol{f}(x) = \mathbf{C}, \tag{6}$$

where

$$\boldsymbol{f}(s) = \begin{pmatrix} \sigma_{xy}(s) \\ \sigma_{yy}(s) \end{pmatrix}, \quad \boldsymbol{A} = \begin{bmatrix} 1 & 0 \\ 0 & 1 \end{bmatrix} = \boldsymbol{I}, \quad \boldsymbol{B} = \begin{bmatrix} 0 & -\beta \\ \beta & 0 \end{bmatrix}, \quad \boldsymbol{C} = \begin{bmatrix} \dfrac{E^* \varepsilon}{2} \\ \dfrac{-E^* x}{2R} \end{bmatrix}. \tag{7}$$

Using Hilbert transform

$$F_k(z) = \frac{1}{2\pi \mathrm{i}} \int_{-a}^{a} \frac{f_k(s)}{s - z} \mathrm{d}s, \quad k = 1, 2, \tag{8}$$

where $z = x + \mathrm{i}y$ and $\mathrm{i} = \sqrt{-1}$, Eq. (6) can be decoupled into two inhomogeneous Hilbert equations to be solved together with boundary conditions

$$\int_{-a}^{a} \sigma_{yy}(x)\mathrm{d}x = -F \quad \int_{-a}^{a} \sigma_{xy}(x)\mathrm{d}x = 0. \tag{9}$$

The solution procedure for this problem is similar to that discussed in Chen and Gao (2006a). Here we skip the details and present only the final solution. The interfacial tractions in the contact region can be expressed in the form

$$\sigma_{yy}(x) + \mathrm{i}\sigma_{xy}(x) = 2\mathrm{i}I(x) + \frac{E^*\beta}{2(1-\beta^2)}\left(\varepsilon + \frac{x\mathrm{i}}{R}\right) - \frac{F(a+x)^{-\bar{r}}(a-x)^{-r}}{\pi}, \tag{10}$$

where

$$I(x) = \frac{-E^*(a+x)^{-\bar{r}}(a-x)^{-r}}{4\pi(1-\beta^2)}\left[\int_{-a}^{a}\left(\varepsilon + \frac{t\mathrm{i}}{R}\right)\frac{(a+t)^{\bar{r}}(a-t)^{r}}{t-x}\mathrm{d}t\right] \tag{11}$$

and r is the stress singularity, κ is the so-called oscillatory index,

$$r = \frac{1}{2} + \mathrm{i}\kappa, \quad \kappa = \frac{1}{2\pi}\ln\frac{1+\beta}{1-\beta}. \tag{12}$$

The associated stress intensity factor can be calculated as

$$K = -\sqrt{2\pi}\lim_{x\to a}(a-x)^r\left[\sigma_{yy}(x) + \mathrm{i}\sigma_{xy}(x)\right] = \frac{-\mathrm{i}E^*(2a)^{-\bar{r}}}{\sqrt{2\pi}(1-\beta^2)}\int_{-a}^{a}\frac{(\varepsilon + \frac{\mathrm{i}t}{R})(a+t)^{\bar{r}}(a-t)^{r}}{a-t}\mathrm{d}t + \frac{\sqrt{2}F(2a)^{-\bar{r}}}{\sqrt{\pi}}, \tag{13}$$

which when substituted into Griffith's condition

$$G = \frac{1}{\cosh^2\pi\kappa}\frac{|K|^2}{2E^*} = \Delta\gamma, \tag{14}$$

leads to the following relationship between the equilibrium contact half-width a, the mismatch strain ε and the external pulling force F,

$$\left|\frac{\mathrm{i}\varepsilon}{2(\beta^2-1)}\left(\frac{a}{R}\right)^{\frac{1}{2}}\int_{-1}^{1}\frac{(1+\xi)^{\bar{r}}(1-\xi)^{r}}{1-\xi}\mathrm{d}\xi + \frac{F}{E^*R}\left(\frac{R}{a}\right)^{\frac{1}{2}} + \frac{1}{2(1-\beta^2)}\left(\frac{a}{R}\right)^{\frac{3}{2}}\int_{-1}^{1}\frac{\xi(1+\xi)^{\bar{r}}(1-\xi)^{r}}{1-\xi}\mathrm{d}\xi\right|^2$$
$$= 2\cosh^2(\pi\kappa)\frac{\pi\Delta\gamma}{E^*R}, \tag{15}$$

where $\Delta\gamma$ denotes the work of adhesion.

4. Non-oscillatory solution

It has been shown that Dundurs' parameter β only plays a minor role in non-slipping adhesive contact (Chen and Gao, 2006a,b,c) and may be neglected for practical purposes. In the case of $\beta = 0$, the tangential and normal tractions inside the contact region are reduced to simpler forms,

$$\sigma_{xy}(x) = \frac{E^*\varepsilon x}{2\sqrt{a^2-x^2}}, \tag{16}$$

$$\sigma_{yy}(x) = \frac{-E^*}{2R}\frac{x^2 - a^2/2}{\sqrt{a^2-x^2}} - \frac{F}{\pi\sqrt{a^2-x^2}}, \tag{17}$$

with stress intensity factors

$$K_{\mathrm{I}} = \frac{E^*\sqrt{\pi}a^{3/2}}{4R} + \frac{F}{\sqrt{\pi a}}, \tag{18}$$

$$K_{\mathrm{II}} = -\frac{E^*\varepsilon\sqrt{\pi a}}{2}. \tag{19}$$

The mode I solution of Eq. (18) is consistent with that given in Chaudhury et al. (1996) and the mode II solution of Eq. (19) is consistent with a similar solution for external crack given in Tada et al. (2000). Inserting Eqs. (18) and (19) into the corresponding Griffith condition in the non-oscillatory case,

$$G = \frac{(K_{\mathrm{I}}^2 + K_{\mathrm{II}}^2)}{2E^*} = \Delta\gamma, \tag{20}$$

leads to the following equation

$$a^3 + 4R^2\varepsilon^2 a + \frac{8RFa}{\pi E^*} - \frac{32\Delta\gamma R^2}{\pi E^*} + \frac{16R^2F^2}{\pi^2 E^{*2} a} = 0, \tag{21}$$

for determining the contact half-width a as a function of the mismatch strain ε and the pulling force F.

In the case of $\varepsilon = 0$, it can be shown that the non-oscillatory solution is identical to the 2D JKR solution of Chaudhury et al. (1996), i.e., $a_{\varepsilon=0} = a_{\mathrm{JKR}}$. In this case, the relationship between the contact size and the pulling force can be expressed as

$$F = \frac{-\pi E^* a_{\mathrm{JKR}}^2}{4R} + \sqrt{2\pi E^* a_{\mathrm{JKR}} \Delta\gamma}. \tag{22}$$

Eq. (21) can be normalized as

$$\hat{a}^3 + 4\lambda^2\varepsilon^2\hat{a} - 1 + 64m^2\left(\frac{1}{\hat{a}} - 1\right) - 16m(1-\hat{a}) = 0, \tag{23}$$

where

$$\hat{a} = \frac{a}{a_{\mathrm{JKR}}}, \quad \lambda = \frac{R}{a_{\mathrm{JKR}}}, \quad m = \frac{FR}{2\pi E^* a_{\mathrm{JKR}}^2}. \tag{24}$$

5. Discussion

5.1. The $\varepsilon = 0$ case

In the case of $\varepsilon = 0$, the stress intensity factor is

$$K = \frac{E^*(2a)^{-\bar{r}}}{\sqrt{2\pi}(1-\beta^2)R}\int_{-a}^{a}\frac{t(a+t)^{\bar{r}}(a-t)^{r}}{a-t}\,\mathrm{d}t + \frac{\sqrt{2}(2a)^{-\bar{r}}F}{\sqrt{\pi}}. \tag{25}$$

Inserting this into the Griffith condition (14) yields

$$\left|\frac{1}{2\sqrt{\pi}(1-\beta^2)}\left(\frac{a_0}{R}\right)^{\frac{3}{2}}\int_{-1}^{1}\frac{\xi(1+\xi)^{\bar{r}}(1-\xi)^{r}}{1-\xi}\mathrm{d}\xi + \left(\frac{R}{a_0}\right)^{\frac{1}{2}}\frac{F}{E^*R\sqrt{\pi}}\right|^2 = 2\cosh^2(\pi\kappa)\frac{\Delta\gamma}{E^*R}, \tag{26}$$

where a_0 denotes the contact size for the case $\varepsilon = 0$. This equation can be normalized as

$$\begin{aligned}&\left|\frac{1}{2\sqrt{\pi}(1-\beta^2)}\tilde{a}^{\frac{3}{2}}\lambda^{-1}\int_{-1}^{1}\frac{\xi(1+\xi)^{\bar{r}}(1-\xi)^{r}}{1-\xi}\mathrm{d}\xi + \tilde{a}^{\frac{1}{2}}\lambda\frac{F}{E^*R\sqrt{\pi}}\right|^2 \\ &\quad = \cosh^2(\pi\kappa)\left[\frac{\pi}{16}\lambda^{-2} + \lambda^2\frac{F^2}{\pi E^{*2}R^2} + \frac{1}{2}\frac{F}{E^*R}\right],\end{aligned} \tag{27}$$

where

$$\tilde{a} = \frac{a_0}{a_{\mathrm{JKR}}}, \quad \lambda = \frac{R}{a_{\mathrm{JKR}}}. \tag{28}$$

Numerical evaluation of (27) indicates that the ratio a_0/a_{JKR} is close to 1. Fig. 2 plots a_0/a_{JKR} for a fixed value of λ and three values of $F/(E^*R)$. It can be seen that the non-oscillatory solution, which for the case $\varepsilon = 0$ corresponds to the JKR model, serves as a good approximate solution to the non-slipping adhesion problem.

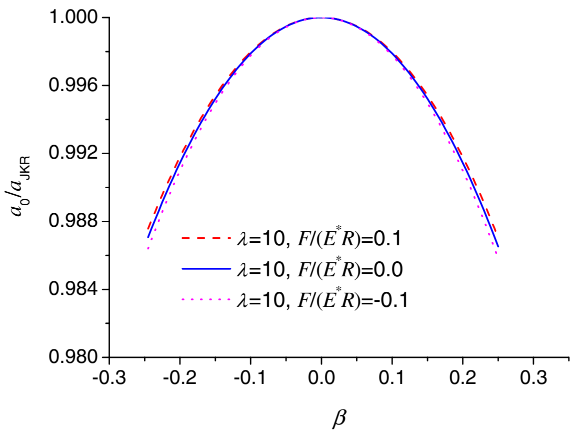

Fig. 2. Effect of shear tractions on contact width in the absence of a mismatch strain. The ratio between a_0, the contact half-width with no slipping along the interface, and a_{JKR}, the contact half-width with no shear tractions along the interface, is plotted as a function of Dundurs' parameter β predicted by Eq. (27) of the text. The result shows that the difference between a_0 and a_{JKR} is less than 2%.

5.2. Effect of mismatch strain

In the presence of a mismatch strain, the coupling between shear and normal tractions in the contact area becomes important. In this case, the contact half-width a is related to the mismatch strain ε and the external force F according to Eq. (15) which can be normalized as

$$\left|\frac{\mathrm{i}\lambda\varepsilon\hat{a}^{\frac{1}{2}}}{2\sqrt{\pi}(\beta^2-1)}\int_{-1}^{1}\frac{(1+\xi)^{\bar{r}}(1-\xi)^{r}}{1-\xi}\mathrm{d}\xi+\frac{\hat{a}^{\frac{3}{2}}}{2\sqrt{\pi}(1-\beta^2)}\int_{-1}^{1}\frac{\xi(1+\xi)^{\bar{r}}(1-\xi)^{r}}{1-\xi}\mathrm{d}\xi+\frac{FR}{\sqrt{\pi}E^*a_0^2\hat{a}^{\frac{1}{2}}}\right|^2$$
$$=\left|\frac{1}{2\sqrt{\pi}(1-\beta^2)}\int_{-1}^{1}\frac{\xi(1+\xi)^{\bar{r}}(1-\xi)^{r}}{1-\xi}\mathrm{d}\xi+\frac{FR}{\sqrt{\pi}E^*a_0^2}\right|^2, \tag{29}$$

where

$$\hat{a}=a/a_0\approx a/a_{\mathrm{JKR}},\quad \lambda=R/a_0\cong R/a_{\mathrm{JKR}}. \tag{30}$$

Numerical evaluation of the above equation indicates that Dundurs' parameter β only plays a minor role and can be neglected so that the non-oscillatory Eq. (23) can be used as a reasonable approximation. An example of comparison between the fully couple solution and the non-oscillatory solution is shown in Fig. 3 for $\beta=0$, 0.25 and -0.25.

The non-oscillatory solution expressed in Eqs. (23) and (24) indicates that, for a given non-dimensional parameter $FR/(2\pi E^*a_{\mathrm{JKR}}^2)$, the normalized contact half-width a/a_{JKR} depends on the mismatch strain ε only through the parameter combination $\lambda\varepsilon$. Fig. 4 plots the relation between a/a_{JKR} and $\lambda\varepsilon$ for several values of the pulling force.

Assuming $\beta=0$, the generalized JKR model for adhesive contact boils down to the following relation

$$F=\frac{-\pi E^*a^2}{4R}+\sqrt{2\pi E^*\Delta\gamma a-\frac{\pi^2E^{*^2}\varepsilon^2a^2}{4}}. \tag{31}$$

Fig. 5 shows the calculated relation between the normalized contact half-width a/R and the normalized external force $F/\Delta\gamma$ for different mismatch strains and a fixed non-dimensional parameter $E^*R/\Delta\gamma$. The mismatch strain is seen to exert significant influence on the pull-off process.

For different values of $E^*R/\Delta\gamma$, Fig. 6 shows the behavior of the normalized pull-off force $F/\Delta\gamma$ as a function of the mismatch strain ε; similarly, Fig. 7 shows the behavior of the normalized critical contact half-width at pull-off. The pull-off force is seen to decrease with increasing mismatch strain. For a given mismatch strain, the normalized pull-off force increases with the non-dimensional parameter $E^*R/\Delta\gamma$. On the other hand, for a

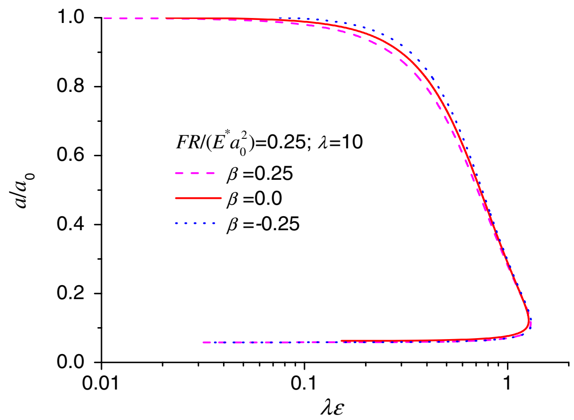

Fig. 3. Variation of normalized contact half-width a/a_0 with $\lambda\varepsilon$ as predicted by Eq. (29) of the text for different values of β and fixed values of $FR/(E^*a_0^2)$ and λ. The results indicate that the influence of β is small and can be neglected.

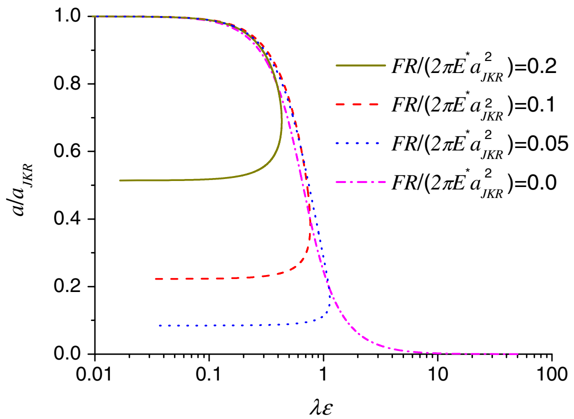

Fig. 4. Variation of a/a_{JKR} via $\lambda\varepsilon$ ($\lambda = R/a_{\mathrm{JKR}}$) for different values of $FR/(2\pi E^* a_{\mathrm{JKR}}^2)$. Under a finite pulling force, the contact size decreases with increasing ε and an instability occurs at a critical value of ε.

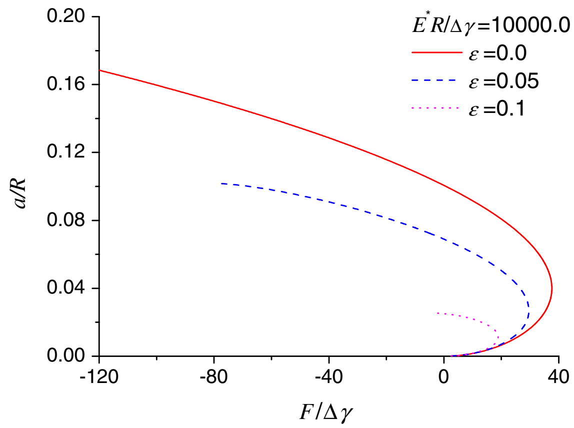

Fig. 5. Normalized contact half-width a/R as a function of the normalized pulling force $F/\Delta\gamma$ for different mismatch strains and a fixed value of $E^*R/\Delta\gamma$.

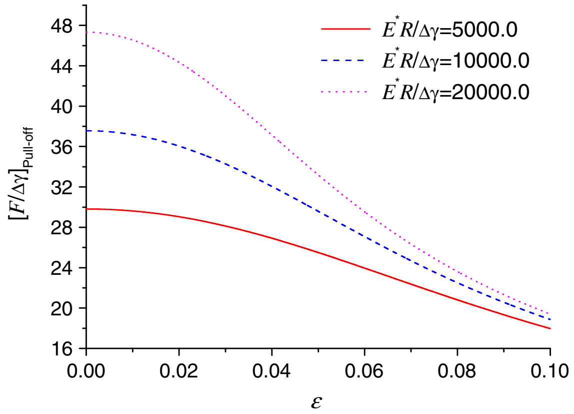

Fig. 6. Normalized pull-off force $F/\Delta\gamma$ as a function of the mismatch strain ε for different values of $E^*R/\Delta\gamma$.

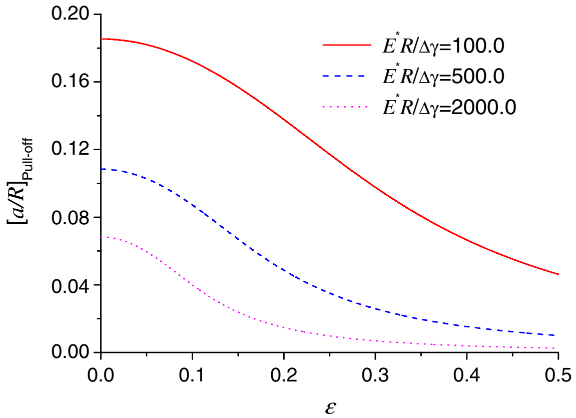

Fig. 7. Normalized critical contact half-width a/R at pull-off as a function of the mismatch strain ε for different values of $E^*R/\Delta\gamma$.

given pulling force, there always exists a critical mismatch strain ε at which two adhering cylinders will spontaneously break apart. Fig. 7 shows that the normalized critical contact half-width a/R at pull-off is also influenced by the mismatch strain: the critical contact width decreases with increasing mismatch strain. For a given mismatch strain, the critical contact width decreases with increasing $E^*R/\Delta\gamma$.

5.3. Adhesion mediated deformation sensor

The present analysis suggests that, under plane strain conditions, two adhering elastic bodies under a pair of pulling forces have an increasing chance to break up in the presence of a mismatch strain. Thermal forces tend to break apart any adhering objects and are therefore analogous to pulling forces considered in the present model. Mismatch strains can be generated by changes in environment pressure or temperature or PH values. These results are similar to our previous analysis with respect to two adhering spheres (Chen and Gao, 2006c).

For a given mismatch strain with no applied pulling force, the adhesion energy can be estimated as

$$\Delta U = \Delta U_{\text{surface}} - \Delta U_{\text{elastic}}, \tag{32}$$

where $\Delta U_{\text{surface}}$ is the change in surface energies and $\Delta U_{\text{elastic}}$ is the change in elastic energy as the contact is formed. These quantities can be calculated as

$$\Delta U_{\text{surface}} = 2a_{\text{eq}}\Delta\gamma, \tag{33}$$

$$\Delta U_{\text{elastic}} = 2\int_0^{a_{\text{eq}}} G|_{\substack{F=0\\ \varepsilon_m\neq 0}}\,\mathrm{d}a, \tag{34}$$

where

$$G|_{\substack{F=0\\ \varepsilon_m\neq}} = \frac{K_{\text{I}}^2 + K_{\text{II}}^2}{2E^*} \tag{35}$$

is the strain energy release rate when $F = 0$, $\varepsilon \neq 0$ and a_{eq} is the corresponding equilibrium contact half-width that can be obtained from Eq. (23) as,

$$a_{\text{eq}} = a_{\text{JKR}}\left[\left(\frac{1}{2} + \sqrt{\frac{1}{4} + \frac{64\lambda^6\varepsilon^6}{27}}\right)^{1/3} - \frac{4\lambda^2\varepsilon^2}{3}\left(\frac{1}{2} + \sqrt{\frac{1}{4} + \frac{64\lambda^6\varepsilon^6}{27}}\right)^{-1/3}\right], \tag{36}$$

where

$$a_{\text{JKR}} = \left[\frac{32R^2\Delta\gamma}{\pi E^*}\right]^{1/3}. \tag{37}$$

The corresponding stress intensity factors can be expressed from Eqs. (18) and (19) as

$$K_{\text{I}} = \frac{E^*\sqrt{\pi}a^{3/2}}{4R}, \quad K_{\text{II}} = -\frac{E^*\varepsilon\sqrt{\pi a}}{2}, \tag{38}$$

Therefore,

$$\Delta U_{\text{elastic}} = \left(\frac{a_{\text{eq}}^2}{8R^2} + \varepsilon^2\right)\frac{\pi E^* a_{\text{eq}}^2}{8}, \tag{39}$$

and the total adhesion energy is

$$\Delta U = 2a_{\text{eq}}\Delta\gamma - \left(\frac{a_{\text{eq}}^2}{8R^2} + \varepsilon^2\right)\frac{\pi E^* a_{\text{eq}}^2}{8}. \tag{40}$$

This result shows explicitly how a mismatch strain decreases that adhesion energy between two adhering bodies. When the adhesion energy is reduced to the order of $k_{\text{B}}T$, adhesion should become unstable against thermal fluctuations.

Acknowledgements

The work reported here was performed under the auspices of the Max Planck Society when HG served as a director at the Max Planck Institute for Metals Research in Stuttgart, Germany, in the last 5 years. S.C. gratefully acknowledges support by a Max Planck Visiting Scientist Fellowship and NSFC (No. 10202023).

References

Artz, E., Gorb, S., Spolenak, R., 2003. From micro to nano contacts in biological attachment devices. Proc. Natl. Acad. Sci. USA 100, 10603–10606.

Autumn, K., Sitti, M., Liang, Y.C., Peattie, A.M., Hansen, W.R., Sponberg, S., Kenny, T.W., Fearing, R., Israelachvili, J.N., Full, R.J., 2002. Evidence for van der Waals adhesion in gecko setae. Proc. Natl. Acad. Sci. USA 99, 12252–12256.

Baney, J.M., Hui, C.Y., 1997. A cohesive zone model for the adhesion of cylinders. J. Adhesion Sci. Technol. 11, 393–406.

Barquins, M., 1988. Adherence and rolling kinetics of a rigid cylinder in contact with a natural rubber surface. J. Adhesion 26, 1–12.

Barthel, E., 1998. On the description of the adhesive contact of spheres with arbitrary interaction potentials. J. Coll. Interface Sci. 200, 7–18.

Carpick, R.W., Agrait, N., Ogletree, D.F., Salmeron, M., 1996. Variation of the interfacial shear strength and adhesion of a nanometer sized contact. Langmuir 12, 3334–3340.

Chaudhury, M.K., Weaver, T., Hui, C.Y., Kramer, E.J., 1996. Adhesion contact of cylindrical lens and a flat sheet. J. Appl. Phys. 80, 30–37.
Chen, S., Gao, H., 2006a. Non-slipping adhesive contact of an elastic cylinder on stretched substrates. Proc. R. Soc. London A 462, 211–228.
Chen, S., Gao, H., 2006b. Generalized Maugis–Dugdale model of an elastic cylinder in non-slipping adhesive contact with a stretched substrate. Int. J. Mat. Res. 97, 584–593.
Chen, S., Gao, H., 2006c. Non-slipping adhesive contact between mismatched elastic spheres: a model of adhesion mediated deformation sensor. J. Mech. Phys. Solids 54, 1548–1567.
Derjaguin, B.V., Muller, V.M., Toporov, Y.P., 1975. Effect of contact deformations on the adhesion of particles. J. Coll. Interface Sci. 53, 314–326.
Dundurs, J., 1969. Edge-bonded dissimilar orthogonal elastic wedges. J. Appl. Mech. 36, 650–652.
Erdogan, F., 1965. Stress distribution in bonded dissimilar materials with cracks. J. Appl. Mech. 32, 403–410.
Gao, H., Yao, H., 2004. Shape insensitive optimal adhesion of nanoscale fibrillar structures. Proc. Natl. Acad. Sci. USA 101, 7851–7856.
Gao, H., Wang, X., Yao, H., Gorb, S., Arzt, E., 2005. Mechanics of hierarchical adhesion structures of gecko. Mech. Mater. 37, 275–285.
Glassmaker, N.J., Jagota, A., Hui, C.Y., Kim, J., 2004. Design of biomimetic fibrillar interface: 1. Making contact. J. R. Soc. Interface 1, 23–33.
Greenwood, J.A., 1997. Adhesion of elastic spheres. Proc. R. Soc. London A 453, 1277–1297.
Greenwood, J.A., Johnson, K.L., 1981. The mechanics of adhesion of viscoelastic solids. Philos. Mag. 43, 697–711.
Greenwood, J.A., Johnson, K.L., 1998. An alterative to the Maugis model of adhesion between elastic spheres. J. Phys. D: Appl. Phys. 31, 3279–3290.
Huber, G., Gorb, S., Spolenak, R., Artz, E., 2005. Resolving the nanoscale adhesion of individual gecko spatulae by atomic force microscopy. Biol. Lett. 1, 2–4.
Hui, C.Y., Glassmaker, N.J., Tang, T., Jagota, A., 2004. Design of biomimetic fibrillar interface: 2. mechanics of enhanced adhesion. J. R. Soc. Interface 1, 35–48.
Johnson, K.L., 1985. Contact Mechanics. Cambridge University Press.
Johnson, K.L., Greenwood, J.A., 1997. An adhesion map for the contact of elastic spheres. J. Coll. Interface Sci. 192, 326–333.
Johnson, K.L., Kendall, K., Roberts, A.D., 1971. Surface energy and the contact of elastic solids. Proc. R. Soc. London A 324, 301–313.
Kim, K.S., McMeeking, R.M., Johnson, K.L., 1998. Adhesion, slip cohesive zone and energy fluxes for elastic spheres in contact. J. Mech. Phys. Solids 46, 243–266.
Maugis, D., 1992. Adhesion of spheres: the JKR–DMT transition using a Dugdale model. J. Coll. Interface Sci. 150, 243–269.
Morrow, C., Lovell, M., Ning, X., 2003. A JKR–DMT transition solution for adhesive rough surface contact. J. Phys. D: Appl. Phys. 36, 534–540.
Muller, V.M., Yushenko, V.S., Derjaguin, B.V., 1980. On the influence of molecular forces on the deformation of an elastic sphere and its sticking to a rigid contact. J. Coll. Interface Sci. 77, 91–101.
Persson, B.N.J., 2003. On the mechanism of adhesion in biological systems. J. Chem. Phys. 118 (16), 7614–7621.
Rice, J.R., 1965. Plane problems of crack in dissimilar media. J. Appl. Mech. 32, 418–423.
Robbe-Valloire, F., Barquins, M., 1998. Adhesive contact and kinetics of adherence between a rigid cylinder and an elastomeric solid. Int. J. Adhes. Adhes. 18, 29–34.
Roberts, A.D., Thomas, A.G., 1975. The adhesion and friction of smooth rubber surfaces. Wear 33, 45–64.
Schwarz, U.D., 2003. A generalized analytical model for the elastic deformation of an adhesive contact between a sphere and a flat surface. J. Coll. Interface Sci. 261, 99–106.
Shull, K.R., 2002. Contact mechanics and the adhesion of soft solids. Mater. Sci. Eng. R – Report 36, 1–45.
Spolenak, R., Gorb, S., Gao, H., Artz, E., 2005. Effects of contact shape on the scaling of biological attachments. Proc. R. Soc. A 461, 305–319.
Tada, H., Paris, P.C., Irwin, G.R., 2000. The stress analysis of cracks handbook, third ed. ASME Press, New York.
Westmann, R.A., 1965. Asymmetric mixed boundary-value problems of the elastic half-space. J. Appl. Mech. 32, 411–417.
Yao, H., Gao, H., 2006. Mechanics of robust and releasable adhesion in biology: bottom-up designed hierarchical structures of gecko. J. Mech. Phys. Solids 54, 1120–1146.